

**Mitigating NO_x emissions does not help alleviate wintertime particulate pollution in
Beijing-Tianjin-Hebei (BTH), China**

Xia Li^{1,5}, Naifang Bei², Bo Hu³, Yuan Wang⁴, Suixin Liu¹, Jiarui Wu¹, Yuepeng Pan³, Tianxue Wen³, Zirui Liu³, Lang Liu¹, Ruonan Wang¹, Min Zuo¹, Zhenxing Shen², Junji Cao^{1,6}, Xuexi Tie¹, Luisa T. Molina⁷, and Guohui Li^{1,6*}

¹Key Lab of Aerosol Chemistry and Physics, SKLLQG, Institute of Earth Environment, Chinese Academy of Sciences, Xi'an, Shaanxi, 710061, China

²School of Human Settlements and Civil Engineering, Xi'an Jiaotong University, Xi'an, Shaanxi, 710049, China

³State Key Laboratory of Atmospheric Boundary Layer Physics and Atmospheric Chemistry, Institute of Atmospheric Physics, Chinese Academy of Sciences, Beijing, 100029, China

⁴Division of Geological and Planetary Sciences, California Institute of technology, Pasadena, CA 91125, USA

⁵University of the Chinese Academy of Sciences, Beijing, 100049, China

⁶CAS Center for Excellence in Quaternary Science and Global Change, Xi'an, Shaanxi, 710061, China

⁷Molina Center for Energy and the Environment, La Jolla, California, CA 92037, USA

* **Correspondence to:** Guohui Li (ligh@ieecas.cn)

Abstract: Stringent mitigation measures have reduced wintertime PM_{2.5} concentrations by 42.2% from 2013 to 2018 in the BTH. The observed nitrate aerosols have not exhibited a significant decreasing trend and constituted a major fraction (about 20%) of the total PM_{2.5}, although the surface-measured NO₂ level has decreased by over 20%. It still remains elusive about contributions of nitrogen oxides (NO_x) emissions mitigation to the nitrate and PM_{2.5} level. The WRF-Chem model simulations of a persistent haze episode in January 2019 in the BTH reveal that NO_x emissions mitigation does not help lower wintertime nitrate and PM_{2.5} concentrations under current conditions in the BTH, because the substantial O₃ increase induced by NO_x mitigation offsets the HNO₃ loss and enhances sulfate and secondary organic aerosols formation. Our results are further consolidated by occurrence of the severe PM pollution in the BTH during the COVID-19 outbreak with a significant reduction of NO₂.

Plain Language Summary: Rapid industrialization and urbanization have caused severe particulate matter (PM) pollution in winter in Beijing-Tianjin-Hebei (BTH) region, China. Strict mitigation measures have been conducted to improve the air quality, but heavy PM pollution still frequently engulfs the region. The observed nitrate aerosols have not exhibited a significant decreasing trend and constituted a major fraction (about 20%) of the PM_{2.5}, although the surface-measured NO₂ level has decreased by over 20%. We quantify the contributions of nitrogen oxides (NO_x) emissions mitigation to the nitrate and PM_{2.5} level in the BTH using a fully coupled WRF-Chem model and further explore how to efficiently alleviate nitrate aerosols under current situations. Our simulations of a persistent heavy haze episode in January 2019 in the BTH reveal that NO_x emissions mitigation does not help lower wintertime nitrate and PM_{2.5} concentrations under current conditions in the BTH and mitigation of NH₃ emissions constitutes the priority measure to effectively decrease the nitrate and PM_{2.5} level.

1. Introduction

The severe and persistent particulate matter (PM) pollution in China is attributed to a synergy of massive anthropogenic emissions and unfavorable synoptic situations, as well as the topography (An et al., 2019; Bei et al., 2016a, b; Long et al., 2016). Great efforts have been made by the Chinese central and local governments to mitigate anthropogenic emissions since 2013 with release of “Air Pollution Prevention and Control Action Plan” (APPCAP) (Li et al., 2019; Zhang et al., 2019). Although anthropogenic emissions of major air pollutants, including sulfur dioxide (SO_2), nitrogen oxides (NO_x), black carbon (BC) and organic carbon (OC) have decreased considerably since 2013 (Zhang et al., 2019; Zheng et al., 2019), persistent and heavy PM pollution still frequently engulfs the Beijing-Tianjin-Hebei (BTH) during wintertime, and observations have revealed that nitrate aerosols concentration has progressively increased in recent several years and constituted a major fraction of $\text{PM}_{2.5}$ in the BTH (Sun et al., 2015; Tao et al., 2017; Zhang et al., 2015). It still remains elusive about the contribution of NO_x emissions mitigation to the nitrate and $\text{PM}_{2.5}$ level.

Nitrate aerosols are formed via nitrous acid (HNO_3) to balance inorganic cations in the particle phase, and the reaction of NO_2 with OH to form HNO_3 and with NO_3 to form N_2O_5 constitute the major HNO_3 formation pathway in the atmosphere (Liu et al., 2019). Hence, the nitrate formation is not only dependent on its precursor (NO_x) and inorganic cations (such as NH_4^+), also significantly influenced by the atmospheric oxidizing capability (AOC) which is mainly determined by O_3 and its photochemical derivative OH, as well as existence of sulfate aerosols (Brasseur et al., 1999; Seinfeld and Pandis, 2006). Therefore, effective mitigation of the nitrate aerosols is still challenging considering the complexity of its formation process.

In the present study, we report analyses of nitrate measurements in the BTH during wintertime, and perform simulations of a persistent and heavy PM pollution episode in

January 2019 using a fully coupled WRF-Chem model to quantitatively estimate contributions of NO_x emissions mitigation to the nitrate and PM_{2.5} level and seek an efficient measure to further alleviate PM pollution in the BTH under current situation.

2. WRF-Chem model and configurations

The WRF-Chem (Weather Research and Forecasting model coupled with Chemistry) model (Fast et al., 2006; Grell et al., 2005) modified by Li et al. (2010; 2011a, b; 2012) is used in the present study to simulate the particulate pollution episode. The wet and dry deposition of aerosols follows the method used in the CMAQ (Community Multiscale Air Quality Model) module (Binkowski and Roselle, 2003) and Wesely (1989), respectively. The photolysis rates are calculated using the FTUV (Fast Radiation Transfer Model), considering both the aerosol and cloud effects on photolysis (Li et al., 2005, 2011b; Tie et al., 2003). The inorganic aerosols are calculated using ISORROPIA (Version 1.7) (Nenes et al., 1998). Besides the SO₂ gas-phase oxidations by OH and sCl, a SO₂ heterogeneous reaction parameterization is adopted in the model, in which the SO₂ oxidation in aerosol water by O₂ catalyzed by Fe³⁺ is limited by mass transfer resistances in the gas-phase and gas-particle interface (Li et al., 2017). The secondary organic aerosol (SOA) is predicted using the volatility basis-set (VBS) modeling method, with contributions from glyoxal and methylglyoxal (Volkamer et al., 2007; Zhao et al., 2006).

In the present study, the WRF-Chem model adopts one grid with horizontal resolution of 6 km (301 × 301 grid points) centered at 38.0°N, 116.0°E (See Figure S1), and 35 sigma vertical levels with a stretched vertical grid with spacing ranging from 30 m near the surface, to 500 m at 2.5 km and 1 km above 14 km. The meteorological initial and boundary conditions are from the NCEP (National Centers for Environmental Prediction) 1° × 1° reanalysis data, and the chemical initial and boundary conditions are interpolated from the 6 h

output of WACCM (Whole Atmosphere Community Climate Model) (Marsh et al., 2013; Neale et al., 2013). The spin-up time of the WRF-Chem model is 100 hours. The SAPRC-99 (Statewide Air Pollution Research Center, version 1999) chemical mechanism is used in simulations. The anthropogenic emission inventory used in this study is developed by Zhang et al. (2009) and Li et al. (2017). The biogenic emissions are calculated online using the MEGAN (Model of Emissions of Gases and Aerosol from Nature) developed by Guenther et al. (2006). More detailed model configurations (Table S1) and monitoring data are provided in *SI Appendix*.

3. Results and discussion

3.1 Variations of air pollutants and aerosol species from 2013 to 2018 in the BTH

Aggressive emission mitigation measures have been carried out in the BTH to decrease air pollutants since implementation of the “Action Plan” in 2013 (Zhang et al., 2019; Zheng et al., 2019). Table 1 shows comparisons of the average mass concentrations of air pollutants during wintertime (referred as to the period from 1 December of the year to 28 February of the next year) in the BTH from 2013 to 2018. The wintertime SO₂ level has been remarkably decreased by around 78.3% from 2013 to 2018, and the average PM_{2.5} concentration has decreased from 153.0 to 88.5 µg m⁻³, or by 42.2%. However, the O₃ concentration displays an increasing trend, with the enhancement of around 30.3%. Besides, NO₂ concentration exhibits a slow decreasing trend compared to SO₂, reduced by about 22.0%.

Although the wintertime PM_{2.5} concentrations in 2018 have decreased substantially compared to that in 2013, the occurrence frequency with daily PM_{2.5} concentrations exceeding 75 µg m⁻³ in the winter of 2018 is about 53.3%, showing persistent particulate pollution in the BTH. Figure 1 shows the variations of the filter measured average concentrations and percentage of the PM_{2.5} constituents at an urban site in Beijing from 2013 to 2018 during wintertime

pollution days with $\text{PM}_{2.5}$ concentrations exceeding $75 \mu\text{g m}^{-3}$. The average wintertime $\text{PM}_{2.5}$ concentration at the site in Beijing decreases from $170.4 \mu\text{g m}^{-3}$ in 2013 to $108.3 \mu\text{g m}^{-3}$ in 2018, reduced by about 36.4% (See Figure S2), which is primarily contributed by decreases in sulfate (51.6%), unspecified constituents (mainly mineral dust, 47.1%), organic aerosols (41.0%), ammonium (37.5%), and nitrate (12.5%). However, the black carbon concentration increases from 2.9 to $4.3 \mu\text{g m}^{-3}$, with an enhancement of 48.3%, which is likely caused by the rapid growth of vehicles in Beijing.

Figure 2 presents variations of wintertime sulfate, nitrate, and ammonium concentrations from 2014 to 2018 in Tianjin, Tangshan, Baoding, and Shijiazhuang in the BTH when the $\text{PM}_{2.5}$ level exceeds $75 \mu\text{g m}^{-3}$. Generally, the wintertime sulfate concentrations exhibit a decreasing trend in the four cities, particularly in Shijiazhuang with the sulfate reduction of about 27.4%. However, the nitrate and ammonium concentrations do not display a decreasing trend, and their contributions to $\text{PM}_{2.5}$ have increased from 11.1% to 18.9% and 5.9% to 10.1% on average in the four cities, respectively (See Figure S3). Due to lack of effective mitigation measures for NH_3 , the NH_3 emissions in China still remain stable since 2010 (Zheng et al., 2019). Therefore, when the metal cation (mainly contained in mineral dust) decreases, NH_3 becomes the dominant contributor of cation to balance anion in the particle phase. Although sulfate aerosols have decreased in the four cities from 2014 to 2018, the ammonium concentration does not decrease or even increase due to decreased competence of metal cation and/or increased nitrate concentrations.

3.2 Contributions of NO_x emissions mitigation to nitrate and $\text{PM}_{2.5}$ level in the BTH

The NO_x emissions have been effectively mitigated since 2013 in China (Zheng et al. 2019) and the observed wintertime NO_2 concentrations have decreased by more than 20% in the BTH from 2013 to 2018 (Table 1). However, nitrate concentrations do not exhibit an evident

decreasing trend in the BTH and have become a major fraction of $\text{PM}_{2.5}$ in the BTH with contributions of around 20% in 2018 (Figure 1b and S3). Therefore, simulations of a persistent and heavy particulate pollution episode from 29 December 2018 to 29 January 2019 in the BTH have been performed using the WRF-Chem model to quantitatively evaluate contributions of NO_x emissions mitigation to nitrate and $\text{PM}_{2.5}$ concentrations and investigate how to effectively alleviate nitrate aerosols. In the base simulation with the emission inventory of the base year of 2018 (F_BASE), the model performs reasonably well in simulating air pollutants ($\text{PM}_{2.5}$, O_3 , NO_2 , and SO_2), sulfate, nitrate, ammonium and organic aerosols and NH_3 . See *SI Appendix* for detailed model validation and quantitative statements of model biases (Figure S4-S7).

Pan et al. (2016b) have redefined the importance of nitrate aerosols during PM pollution and indicated that controlling NO_x emissions should be a priority in mitigating the serious air pollution. Previous studies have also shown that decreasing NO_x might represent a positive feedback mechanism to reduce the conversion of primary gas pollutants into secondary aerosols (He et al., 2014; Ma et al., 2010; Xu et al., 2015; Wang et al., 2014). Therefore, a sensitivity simulation is firstly conducted in the present study, in which the NO_x emission in the base year of 2013 is used (F_EM13). Compared to F_EM13, on average in the BTH, the NO_2 concentration in F_BASE decreases by around 17.1% but the O_3 concentration increases by 44.2%, which is generally consistent with the observed NO_2 and O_3 trend from 2013 to 2018 (Table 1). However, the average $\text{PM}_{2.5}$ concentration in F_BASE is $91.8 \mu\text{g m}^{-3}$, 2.9% higher than that in F_EM13 (Figure 3a). The $\text{PM}_{2.5}$ enhancement in F_BASE against F_EM13 is contributed by the increase in secondary aerosols, i.e., sulfate ($0.5 \mu\text{g m}^{-3}$), nitrate ($0.9 \mu\text{g m}^{-3}$), ammonium ($0.3 \mu\text{g m}^{-3}$), and SOA ($0.9 \mu\text{g m}^{-3}$).

In order to further assess the impact of NO_x emissions mitigation on the nitrate and $\text{PM}_{2.5}$ level in the BTH, the first sensitivity scenario is designed, in which the NO_x emission in

F_BASE is reduced from 10% to 50% with a 10% interval. As shown in Figure 3a, the variations in PM_{2.5} concentration are not as expected, with an average enhancement of about 3.2% (3.0 $\mu\text{g m}^{-3}$) in the BTH when NO_x emissions are reduced by 50%. Although the NO₂ level is decreased monotonically from 6.4% to 40.0% in the BTH with NO_x emissions decreased from 10% to 50% (Figure 3b), the nitrate concentration increases by 1.1% and then decreases by 10.3%. Additionally, the SOA, sulfate, and ammonium concentrations are increased from 3.3% to 10.9%, 4.4% to 26.7%, and 1.9% to 6.3% in the BTH, respectively (Figure 3a).

Therefore, mitigation of NO_x emissions is not beneficial to the air quality at present during wintertime in the BTH (Figure 3c-3d). Decreasing NO_x emissions does not proportionally reduce the nitrate concentrations, and particularly enhances formation of sulfate, ammonium, and SOA, which is primarily caused by the increase in O₃ concentrations (Figure 3b). In winter in the BTH, the weak insolation significantly decrease photolysis and slow the O₃ formation. During PM pollution period, the lower atmosphere is stable or stagnant, which is quite favorable for accumulation of air pollutants. The titration of NO_x (mainly NO) emissions remarkably influence the O₃ level in the PBL. Figure S8 shows the variations of observed O₃ and NO₂ concentrations as a function of the PM_{2.5} level over all the monitoring sites in the BTH during the wintertime from 2013 to 2018. With deterioration of PM pollution, the O₃ concentration decreases but it is opposite for the NO₂ concentration. Therefore, when the NO_x emissions are decreased from 10% to 50%, the O₃ concentration is increased from 11.8% to 83.8% in the BTH (Figure 3b). Increased O₃ concentrations enhance the AOC, not only promoting the SOA and sulfate formation, but also accelerating conversion of NO₂ to HNO₃ to counterbalance HNO₃ decrease due to mitigation of NO_x emissions. Our results on contributions of NO_x emission mitigation to PM_{2.5} concentrations are also supported by occurrence of the severe PM pollution in the BTH during outbreak of the

Coronavirus Disease 2019 (COVID-19) pandemic with a significant reduction of NO₂. Due to the outbreak of COVID-19, the nationwide preventive lockdown has been carried out since late January 2020 in China, by shutdown of commercial activities and restrictions of population movement. The nationwide lockdown has lasted for more than three weeks and caused remarkable reductions in emissions of air pollutants (Huang et al., 2020; Le et al., 2020; Shi and Brasseur, 2020). Observations from the Tropospheric Monitoring Instrument (TROPOMI) have shown a more than 70% decrease of the column-integrated NO₂ amount during the lockdown period in 2020 over eastern China, compared to that in the same time period in 2019 (Le et al., 2020). Surface measurements have also revealed that the NO₂ concentrations have decreased by about 60% between the period 1-22 January 2020 and the period 23 January-29 February 2020 in northern China (Shi and Brasseur, 2020). However, several severe PM pollution events have still occurred in the BTH, with the maximum daily PM_{2.5} concentration exceeding 250 µg m⁻³ in Beijing, although the observed NO₂ level has decreased substantially. Therefore, additional two sensitivity experiments have been devised based on F_BASE, in which the NO_x emissions are further decreased by 60% and 80% to represent variations of the NO_x emission mitigation during the lockdown period. When the NO_x emissions are decreased from 60% to 80%, the NO₂ concentrations in the BTH are reduced from 51.0% to 75.7% compared to those in F_BASE (Figure 3a), which is within the range of the observed NO₂ variation due to the nationwide lockdown. However, the PM_{2.5} level is increased by 2.2% with a 60% reduction of NO_x emissions and decreased by 3.2% with an 80% reduction of NO_x emissions (Figure 3a), showing the significant NO_x emissions reduction does not help lower the PM_{2.5} level during the lockdown period in the BTH. The main reason is that the substantial increase in O₃ concentrations (more than 100%) causes enhancement of SOA and sulfate to offset the nitrate loss.

3.3 Priority measure to alleviate wintertime PM pollution in the BTH under current situation

Apparently, mitigation of NO_x emissions alleviates O₃ titration during wintertime in the BTH, increasing O₃ concentrations and further the AOC to enhance formation of secondary aerosols. Therefore, decreasing the AOC might effectively lower the nitrate and PM_{2.5} level in the BTH. The second sensitivity scenario is therefore designed, in which the VOCs emission in F_BASE is reduced from 10% to 50% with a 10% interval to lower the O₃ concentration. With a 50% reduction of VOCs emissions, the O₃ concentration is decreased by 19.6% in the BTH (See Figure S9b), showing considerable weakening of the AOC. However, the decreases in sulfate, nitrate, and ammonium concentrations are not substantial, only about 13.0%, 18.6%, and 6.1%, respectively (See Figure S9a). The SOA concentration is decreased by about 37.6%, caused to a large degree by the reduction of SOA precursors. Overall, the decrease in PM_{2.5} concentration is not significant (See Figure S9c-9d), around 6.9% (6.3 μg m⁻³) in the BTH, when VOCs emissions are reduced by 50%.

As a large agricultural country, China produces a huge amount of NH₃ emissions, with agricultural activities accounting for more than 80% (Huang et al., 2012; Paulot et al., 2014; Zhang et al., 2018). Recent studies have pointed out that NH₃ plays an important role in the PM_{2.5} formation and NH₃ control has been advocated as a potential measure by policy makers, given that atmospheric NH₃ facilitates secondary inorganic aerosol formation, i.e., ammonium sulfate/bisulfate and ammonium nitrate (Fu et al., 2017; Guo et al., 2018; Weber, et al., 2016). Figure S9 presents the pattern comparisons of simulated and measured near-surface NH₃ mass concentrations averaged during January 2019. Compared with measurements, the WRF-Chem model reasonably well simulates the spatial distributions of the NH₃ mass concentrations in the BTH. The NH₃ level is quite high in the plain region of the BTH, with mass concentrations exceeding 5 μg m⁻³. It is well known that the major

source of NH_3 is agricultural activities, mainly including livestock and fertilizer use (Huang et al., 2012; Streets et al., 2003). Additionally, nonagricultural sources (e.g., vehicles, coal combustion, etc.) are also responsible for the high NH_3 emissions in China, especially in urban areas (Chang et al., 2016; Pan et al., 2016a).

Thus, we have further performed the third sensitivity scenario, in which the NH_3 emission in F_BASE is reduced from 10% to 50% with a 10% interval. With a 50% reduction of NH_3 emissions, the nitrate and ammonium concentrations are decreased by 34.5% and 36.5% in the BTH (Figure 4a), respectively. The sulfate concentrations are also reduced by 6.5%, which is mainly caused by the loss of aerosol liquid water due to decrease in nitrate and ammonium aerosols (Wu et al., 2019). The SOA concentration in the BTH is slightly decreased by 0.1% when the NH_3 emissions are reduced by 10% and then increased from 0.1% to 0.6% when the NH_3 emissions are reduced from 20% to 50%. The $\text{PM}_{2.5}$ decrease is about 12.3% ($11.3 \mu\text{g m}^{-3}$) in the BTH (Figure 4c-4d), when NH_3 emissions are reduced by 50%, showing mitigating NH_3 emissions is much more effective to reduce PM pollution in the BTH than NO_x and VOCs emissions.

4. Conclusions

The Chinese government has made great efforts to mitigate emissions of primary PM, SO_2 and NO_x to alleviate PM pollution since 2013. The observed near-surface wintertime concentrations of $\text{PM}_{2.5}$, SO_2 , and NO_2 have decreased by 42.2%, 78.3% and 22.0% from 2013 to 2018 in the BTH, respectively, but persistent PM pollution still frequently occurs. Observations show that nitrate aerosols have not exhibited a significant decreasing trend and play an increasing role in PM pollution during wintertime in the BTH, with a $\text{PM}_{2.5}$ contribution of about 20%. Our sensitivity simulations of a persistent heavy PM pollution episode in January 2019 in the BTH reveal that NO_x emissions mitigation does not help

lower nitrate and PM_{2.5} concentrations during wintertime. A 50% reduction of NO_x emissions only decreases nitrate mass by 10.3% but increases PM_{2.5} concentrations by around 3.2% because the O₃ increase induced by NO_x mitigation offsets the loss of HNO₃ and enhances sulfate and SOA formation. Our results are also consolidated by occurrence of server PM pollutions in the BTH during the COVID-19 outbreak when the NO_x emissions have been remarkably reduced and the observed NO₂ level has decreased by more than 60%. Although the emissions reduction of VOCs has been proposed to be particularly important to mitigate PM pollution, our results reveal that a 50% reduction in VOCs emissions decreases PM_{2.5} concentrations by around 7% in the BTH. However, when NH₃ emissions are reduced by 50%, the PM_{2.5} level is decreased by about 12%, mainly caused by substantial decreases in nitrate and ammonium aerosols. Therefore, we suggest that, in addition to primary PM emissions, mitigating NH₃ emissions is the priority measure to effectively alleviate PM pollution during wintertime in the BTH under the current situation.

Acknowledgments. This work is financially supported by the Strategic Priority Research Program of Chinese Academy of Sciences (XDB40030203), the National Key R&D Plan (2017YFC0210000), and National Research Program for Key Issues in Air Pollution Control (DQGG0105).

References

- An, Z. S., Huang, R. J., Zhang, R. Y., Tie, X. X., Li, G. H., Cao, J. J., et al. (2019) Severe haze in northern China: A synergy of anthropogenic emissions and atmospheric processes. *Proceedings of the National Academy of Sciences of the United States of America*, 116(18), 8657-8666. <https://doi.org/10.1073/pnas.1900125116>
- Bei, N. F., Li, G. H., Huang, R. J., Cao, J. J., Meng, N., Feng, T., et al. (2016a) Typical synoptic situations and their impacts on the wintertime air pollution in the Guanzhong basin, China. *Atmospheric Chemistry and Physics*, 16(11), 7373-7387. <https://doi.org/10.5194/acp-16-7373-2016>
- Bei, N. F., Xiao, B., Meng, N., & Feng, T. (2016b) Critical role of meteorological conditions in a persistent haze episode in the Guanzhong basin, China. *Science of the Total Environment*, 550, 273-284. <https://doi.org/10.1016/j.scitotenv.2015.12.159>
- Binkowski, F. S., & Roselle, S. J. (2003) Models-3 Community Multiscale Air Quality (CMAQ) model aerosol component 1. Model description. *Journal of Geophysical Research*, 108(D6), 4183. <https://doi.org/10.1029/2001JD001409>
- Brasseur, G. P., Orlando, J. J., & Tyndall, G. S. (1999) *Atmospheric Chemistry and Global Change*. Cambridge, MA: Oxford University Press. <https://doi.org/10.1029/EO080i040p00468-02>
- Chang, Y. H., Zou, Z., Deng, C. R., Huang, K., Collett, J. L., Lin, J., & Zhuang, G. S. (2016) The importance of vehicle emissions as a source of atmospheric ammonia in the megacity of Shanghai. *Atmospheric Chemistry and Physics*, 16(5), 3577-3594. <https://doi.org/10.5194/acp-16-3577-2016>
- Elser, M., Huang, R., Wolf, R., Slowik, J. G., Wang, Q., Canonaco, F., et al. (2016) New insights into PM_{2.5} chemical composition and sources in two major cities in China during extreme haze events using aerosol mass spectrometry. *Atmospheric Chemistry and Physics*, 16(5), 3207-3225. <https://doi.org/10.5194/acp-16-3207-2016>
- Fast, J. D., Jr, W. I. G., Easter, R. C., Zaveri, R. A., Barnard, J. C., Chapman, E. G., et al. (2006) Evolution of ozone, particulates, and aerosol direct radiative forcing in the vicinity of Houston using a fully coupled meteorology-chemistry-aerosol model. *Journal of Geophysical Research-Atmospheres*, 111(D21), D21305. <https://doi.org/10.1029/2005JD006721>
- Fu, X., Wang, S. X., Xing, J., Zhang, X. Y., Wang, T., & Hao, J. M. (2017) Increasing Ammonia Concentrations Reduce the Effectiveness of Particle Pollution Control Achieved via SO₂ and NO_x Emissions Reduction in East China. *Environmental Science & Technology Letters*, 4(6), 221-227. <https://doi.org/10.1021/acs.estlett.7b00143>
- Gao, M., Carmichael, G. R., Wang, Y., Saide, P. E., Yu, M., Xin, J., et al. (2016) Modeling study of the 2010 regional haze event in the North China Plain. *Atmospheric Chemistry and Physics*, 16(3), 1673-1691. <https://doi.org/10.5194/acp-16-1673-2016>
- Grell, G. A., Peckham, S. E., Schmitz, R., McKeen, S. A., Frost, G., Skamarock, W. C., & Eder, B. (2005) Fully coupled "online" chemistry within the WRF model. *Atmospheric Environment*, 39(37), 6957-6975. <https://doi.org/10.1016/j.atmosenv.2005.04.027>
- Guenther, A., Karl, T., Harley, P., Wiedinmyer, C., Palmer, P. I., & Geron, C. (2006) Estimates of global terrestrial isoprene emissions using MEGAN (Model of Emissions of Gases and Aerosols from Nature). *Atmospheric Chemistry and Physics*, 6, 3181-3210. <https://doi.org/10.5194/acp-6-3181-2006>
- Guo, H., Otjes, R., Schlag, P., Kiendler-Scharr, A., Nenes, A., & Weber, R. J. (2018) Effectiveness of ammonia reduction on control of fine particle nitrate. *Atmospheric Chemistry and Physics*, 18(16), 12241-12256. <https://doi.org/10.5194/acp-18-12241-2018>
- Guo, S., Hu, M., Zamora, M. L., Peng, J., Shang, D., Zheng, J., et al. (2014) Elucidating severe urban haze formation in China. *Proceedings of the National Academy of Sciences of the United States of America*,

337 111(49), 17373-17378. <https://doi.org/10.1073/pnas.1419604111>

338 He, H., Wang, Y., Ma, Q., Ma, J., Chu, B., Ji, D., et al. (2014) Mineral dust and NO_x promote the
339 conversion of SO₂ to sulfate in heavy pollution days. *Scientific Reports*, 4, 4172.
340 <https://doi.org/10.1038/srep04172>

341 Huang, R. J., Zhang, Y., Bozzetti, C., Ho, K. F., Cao, J. J., Han, Y. M., et al. (2014) High secondary aerosol
342 contribution to particulate pollution during haze events in China. *Nature*, 514(7521), 218-222.
343 <https://doi.org/10.1038/nature13774>

344 Huang, X., Ding, A. J., Gao, J., Zheng, B., Zhou, D. R., Qi, X. M., et al. (2020) Enhanced secondary
345 pollution offset reduction of primary emissions during COVID-19 lockdown in China. *National*
346 *Science Review*, nwaal37. <https://doi.org/10.31223/osf.io/hvuzy>

347 Huang, X., Song, Y., Li, M. M., Li, J. F., Huo, Q., Cai, X. H., et al. (2012) A high-resolution ammonia
348 emission inventory in China. *Global Biogeochemical Cycles*, 26, GB1030.
349 <https://doi.org/10.1029/2011GB004161>

350 Le, T. H., Wang, Y., Liu, L., Yang, J. N., Yung, Y. L., Li, G. H., & Seinfeld, J. H. (2020) Unexpected air
351 pollution with marked emission reductions during the COVID-19 outbreak in China. *Science*,
352 369(6504), 702-706. <https://doi.org/10.1126/science.abb7431>

353 Li, G. H., Bei, N. F., Cao, J. J., Huang, R. J., Wu, J. R., Feng, T., et al. (2017) A possible pathway for rapid
354 growth of sulfate during haze days in China. *Atmospheric Chemistry and Physics*, 17(5), 3301-3316.
355 <https://doi.org/10.5194/acp-17-3301-2017>

356 Li, G. H., Bei, N. F., Tie, X. X., & Molina, L. T. (2011a) Aerosol effects on the photochemistry in Mexico
357 City during MCMA-2006/MILAGRO campaign. *Atmospheric Chemistry and Physics*, 11(11),
358 5169-5182. <https://doi.org/10.5194/acp-11-5169-2011>

359 Li, G. H., Lei, W. F., Bei, N. F., & Molina, L. T. (2012) Contribution of garbage burning to chloride and
360 PM_{2.5} in Mexico City. *Atmospheric Chemistry and Physics*, 12(18), 8751-8761.
361 <https://doi.org/10.5194/acp-12-8751-2012>

362 Li, G. H., Lei, W. F., Zavala, M., Volkamer, R., Dusanter, S., Stevens, P., & Molina, L. T. (2010) Impacts
363 of HONO sources on the photochemistry in Mexico City during the MCMA-2006/MILAGO
364 Campaign. *Atmospheric Chemistry and Physics*, 10(14), 6551-6567.
365 <https://doi.org/10.5194/acp-10-6551-2010>

366 Li, G. H., Zavala, M., Lei, W. F., Tsimpidi, A. P., Karydis, V. A., Pandis, S. N., et al. (2011b) Simulations
367 of organic aerosol concentrations in Mexico City using the WRF- CHEM model during the
368 MCMA-2006/MILAGRO campaign. *Atmospheric Chemistry and Physics*, 11(8), 3789-3809.
369 <https://doi.org/10.5194/acp-11-3789-2011>

370 Li, G. H., Zhang, R. Y., Fan, J., & Tie, X. X. (2005) Impacts of black carbon aerosol on photolysis and
371 ozone. *Journal of Geophysical Research-Atmospheres*, 110(D23), D23206.
372 <https://doi.org/10.1029/2005JD005898>

373 Li, K., Jacob, D. J., Liao, H., Zhu, J., & Zhai, S. (2019) A two-pollutant strategy for improving ozone and
374 particulate air quality in China. *Nature Geoscience*, 12(11).
375 <https://doi.org/10.1038/s41561-019-0464-x>

376 Li, M., Zhang, Q., Kurokawa, J. I., Woo, J. H., He, K., Lu, Z., et al. (2017) MIX: a mosaic Asian
377 anthropogenic emission inventory under the international collaboration framework of the MICS-Asia
378 and HTAP. *Atmospheric Chemistry and Physics*, 17(2), 935-963.
379 <https://doi.org/10.5194/acp-17-935-2017>

380 Liu, L., Wu, J. R., Liu, S. X., Li, X., Zhou, J. M., Feng, T., et al. (2019) Effects of organic coating on the
381 nitrate formation by suppressing the N₂O₅ heterogeneous hydrolysis: a case study during wintertime
382 in Beijing-Tianjin-Hebei (BTH). *Atmospheric Chemistry and Physics*, 19(12), 8189-8207.

383 <https://doi.org/10.5194/acp-19-8189-2019>

384 Liu, W. J., Shen, G. F., Chen, Y. C., Shen, H. Z., Huang, Y., Li, T. C., et al. (2018) Air pollution and
 385 inhalation exposure to particulate matter of different sizes in rural households using improved stoves
 386 in central China. *Journal of Environmental Science*, 63, 87-95.
 387 <https://doi.org/10.1016/j.jes.2017.06.019>

388 Long, X., Tie, X., Cao, J., Huang, R., Feng, T., Li, N., et al. (2016) Impact of crop field burning and
 389 mountains on heavy haze in the North China Plain: a case study. *Atmospheric Chemistry and Physics*,
 390 16(15), 9675-9691. <https://doi.org/10.5194/acp-16-9675-2016>

391 Ma, Q., He, H., & Liu, Y. (2010) In situ DRIFTS study of hygroscopic behavior of mineral aerosol.
 392 *Journal of Environmental Science*, 22(4), 555-560. [https://doi.org/10.1016/S1001-0742\(09\)60145-5](https://doi.org/10.1016/S1001-0742(09)60145-5)

393 Marsh, D. R., Mills, M., Kinnison, D., Lamarque, J. F., Calvo, N., & Polvani, L. (2013) Climate change
 394 from 1850 to 2005 simulated in CESM1(WACCM). *Journal of Climate*, 26(19), 7372-7391.
 395 <https://doi.org/10.1175/JCLI-D-12-00558.1>

396 Neale, R. B., Richter, J., Park, S., Lauritzen, P. H., Vavrus, S. J., Rasch, P. J., & Zhang, M. (2013) The
 397 Mean Climate of the Community Atmosphere Model (CAM4) in Forced SST and Fully Coupled
 398 Experiments. *Journal of Climate*, 26(14), 5150-5168. <https://doi.org/10.1175/JCLI-D-12-00236.1>

399 Nenes, A., Pandis, S. N., & Pilinis, C. (1998) ISORROPIA: A new thermodynamic equilibrium model for
 400 multiphase multi-component inorganic aerosols. *Aquatic Geochemistry*, 4, 123-152.

401 Pan, Y. P., Tian, S. L., Liu, D. W., Fang, Y. T., Zhu, X. Y., Zhang, Q., et al. (2016a) Fossil Fuel
 402 Combustion-Related Emissions Dominate Atmospheric Ammonia Sources during Severe Haze
 403 Episodes: Evidence from N-15-Stable Isotope in Size-Resolved Aerosol Ammonium. *Environmental*
 404 *Science & Technology*, 50(15), 8049-8056. <https://doi.org/10.1021/acs.est.6b00634>

405 Pan, Y. P., Wang, Y. S., Zhang, J. K., Liu, Z. R., Wang, L. L., Tian, S. L., et al. (2016b) Redefining the
 406 importance of nitrate during haze pollution to help optimize an emission control strategy. *Atmospheric*
 407 *Environment*, 141, 197-202. <https://doi.org/10.1016/j.atmosenv.2016.06.035>

408 Paulot, F., Jacob, D. J., Pinder, R. W., Bash, J. O., Travis, K., & Henze, D. K. (2014) Ammonia emissions
 409 in the United States, European Union, and China derived by high-resolution inversion of ammonium
 410 wet deposition data: Interpretation with a new agricultural emissions inventory (MASAGE_NH₃).
 411 *Journal of Geophysical Research-Atmospheres*, 119(7), 4343-4364.
 412 <https://doi.org/10.1002/2013JD021130>

413 Seinfeld, J. H., & Pandis, S. N. (2006) *Atmospheric Chemistry and Physics: From Air Pollution to Climate*
 414 *Change*, 2nd Edition. New York: John Wiley and Sons Inc. <https://doi.org/10.1063/1.882420>

415 Shi, X. Q., & Brasseur, G. P. (2020) The Response in Air Quality to the Reduction of Chinese Economic
 416 Activities During the COVID-19 Outbreak. *Geophysical Research Letters*, 47(11).
 417 <https://doi.org/10.1029/2020GL088070>

418 State Council of the People's Republic of China, Notice of the general office of the state council on issuing
 419 the air pollution prevention and control action plan.
 420 http://www.gov.cn/zwzk/2013-09/12/content_2486773.htm. Accessed 4 August 2020.

421 Streets, D. G., Bond, T. C., Carmichael, G. R., Fernandes, S. D., Fu, Q., He, D., et al. (2003) An inventory
 422 of gaseous and primary aerosol emissions in Asia in the year 2000. *Journal of Geophysical Research*,
 423 108(D21), 8809. <https://doi.org/10.1029/2002JD003093>

424 Sun, Y. L., Wang, Z. F., Du, W., Zhang, Q., Wang, Q. Q., Fu, P. Q., et al. (2015) Long-term real-time
 425 measurements of aerosol particle composition in Beijing, China: seasonal variations, meteorological
 426 effects, and source analysis. *Atmospheric Chemistry and Physics*, 15(17), 10149-10165.
 427 <https://doi.org/10.5194/acp-15-10149-2015>

428 Tao, J., Zhang, L., Cao, J. J., & Zhang, R. Y. (2017) A review of current knowledge concerning PM_{2.5}
429 chemical composition, aerosol optical properties and their relationships across China. *Atmospheric*
430 *Chemistry and Physics*, 17(15), 9485-9518. <https://doi.org/10.5194/acp-17-9485-2017>

431 Tie, X. X., Madronich, S., Walters, S., Zhang, R. Y., Rasch, P., & Collins, W. (2003) Effect of clouds on
432 photolysis and oxidants in the troposphere. *Journal of Geophysical Research*, 108(D20), 4642.
433 <https://doi.org/10.1029/2003JD003659>

434 Volkamer, R., San Martini, F., Molina, L. T., Salcedo, D., Jimenez, J. L., & Molina, M. J. (2007) A missing
435 sink for gas-phase glyoxal in Mexico City: formation of secondary organic aerosol. *Geophysical*
436 *Research Letters*, 34(19), L19807. <https://doi.org/10.1029/2007GL030752>

437 Wang, G. H., Zhang, R. Y., Gomez, M. E., Yang, L. X., Zamora, M. L., Hu, M., et al. (2016) Persistent
438 sulfate formation from London Fog to Chinese haze. *Proceedings of the National Academy of*
439 *Sciences of the United States of America*, 113(48), 13630-13635.
440 <https://doi.org/10.1073/pnas.1616540113>

441 Wang, Y., Yao, L., Wang, L., Liu, Z., Ji, D., Tang, G., et al. (2014) Mechanism for the formation of the
442 January 2013 heavy haze pollution episode over central and eastern China. *Science China-Earth*
443 *Science*, 57(1), 14-25. <https://doi.org/10.1007/s11430-013-4773-4>

444 Weber, R. J., Guo, H. Y., Russell, A. G., & Nenes, A. (2016) High aerosol acidity despite declining
445 atmospheric sulfate concentrations over the past 15 years. *Nature Geoscience*, 9(4), 282-285.
446 <https://doi.org/10.1038/NGEO2665>

447 Wei, S. Y., Shen, G. F., Zhang, Y. Y., Xue, M., Xie, H., Lin, P. C., et al. (2014) Field measurement on the
448 emissions of PM, OC, EC and PAHs from indoor crop straw burning in rural China. *Environmental*
449 *Pollution*, 184(SI), 18-24. <https://doi.org/10.1016/j.envpol.2013.07.036>

450 Wesely, M. L. (1989) Parameterization of surface resistances to gaseous dry deposition in regional-scale
451 numerical models. *Atmospheric Environment*, 23(6), 1293-1304.
452 [https://doi.org/10.1016/0004-6981\(89\)90153-4](https://doi.org/10.1016/0004-6981(89)90153-4)

453 Wu, J. R., Bei, N. F., Hu, B., Liu, S. X., Zhou, M., Wang, Q. Y., et al. (2019) Is water vapor a key player of
454 the wintertime haze in North China Plain? *Atmospheric Chemistry and Physics*, 19(13), 8721-8739.
455 <https://doi.org/10.5194/acp-2018-1289>

456 Xu, W., Luo, X. S., Pan, Y. P., Zhang, L., Tang, A. H., Shen, J. L., et al. (2015) Quantifying atmospheric
457 nitrogen deposition through a nationwide monitoring network across China. *Atmospheric Chemistry*
458 *and Physics*, 15(21), 12345-12360. <https://doi.org/10.5194/acp-15-12345-2015>

459 Zhang L, Chen, Y. F., Zhao, Y. H., Henze, D. K., Zhu, L. Y., Song, Y., et al. (2018) Agricultural ammonia
460 emissions in China: Reconciling bottom-up and top-down estimates. *Atmospheric Chemistry and*
461 *Physics*, 18(1), 339-355. <https://doi.org/10.5194/acp-18-339-2018>

462 Zhang, Q., He, K. B., & Huo, H. (2012) Policy: Cleaning China's air. *Nature*, 484(7393), 161-162.
463 <https://doi.org/10.1038/484161a>

464 Zhang, Q., Streets, D. G., & Carmichael, G. R. (2009) Asian emissions in 2006 for the NASA INTEX-B
465 mission. *Atmospheric Chemistry and Physics*, 9(14), 5131-5153.
466 <https://doi.org/10.5194/acp-9-5131-2009>

467 Zhang, Q., Zheng, Y. X., Tong, D., Shao, M., Wang, S. X., Zhang, Y. H., et al. (2019) Drivers of improved
468 PM_{2.5} air quality in China from 2013 to 2017. *Proceedings of the National Academy of Sciences of the*
469 *United States of America*, 116(49), 24463-24469. <https://doi.org/10.1073/pnas.1907956116>

470 Zhang, R. Y., Li, G. H., Fan, J. W., Wu, D. L., & Molina, M. J. (2007) Intensification of Pacific storm track
471 linked to Asian pollution. *Proceedings of the National Academy of Sciences of the United States of*
472 *America*, 104(13), 5295-5299. <https://doi.org/10.1073/pnas.0700618104>

473 Zhang, R. Y., Wang, G. H., Guo, S., Zamora, M. L., Ying, Q., Lin, Y., et al. (2015) Formation of urban fine
474 particulate matter. *Chemical Reviews*, 115(10), 3803-3855.
475 <https://doi.org/10.1021/acs.chemrev.5b00067>

476 Zhao, B., Wu, W. J., Wang, S. X., Xing, J., Chang, X., Liou, K. N., et al. (2017) A modeling study of the
477 nonlinear response of fine particles to air pollutant emissions in the Beijing-Tianjin-Hebei region.
478 *Atmospheric Chemistry and Physics*, 17(19), 12031-12050.
479 <https://doi.org/10.5194/acp-17-12031-2017>

480 Zhao, J., Levitt, N. P., Zhang, R., & Chen, J. (2006) Heterogeneous reactions of methylglyoxal in acidic
481 media: implications for secondary organic aerosol formation. *Environmental Science & Technology*,
482 40(24), 7682-7687. <https://doi.org/10.1021/es060610k>

483 Zheng, H., Kong, S. F., Wu, F. Q., Cheng, Y., Niu, Z. Z., Zheng, S. R., et al. (2019) Intra-regional transport
484 of black carbon between the south edge of the North China Plain and central China during winter
485 haze episodes. *Atmospheric Chemistry and Physics*, 19(7), 4499-4516.
486 <https://doi.org/10.5194/acp-19-4499-2019>

487

Table 1. Comparisons of the average mass concentrations of air pollutants during wintertime in the BTH from 2013 and 2018.

Air pollutants	PM _{2.5} (µg m ⁻³)	O ₃ (µg m ⁻³)	NO ₂ (µg m ⁻³)	SO ₂ (µg m ⁻³)	CO (mg m ⁻³)
2013	153.0	37.9	69.2	108.7	2.6
2014	112.0	42.4	60.3	82.2	2.4
2015	106.8	43.4	63.3	58.3	2.4
2016	136.9	48.2	71.8	52.0	2.6
2017	78.7	47.6	50.6	28.8	1.5
2018	88.5	49.4	54.0	23.6	1.5
Change (%) between 2013 and 2018	-42.2	30.3	-22.0	-78.3	-42.3

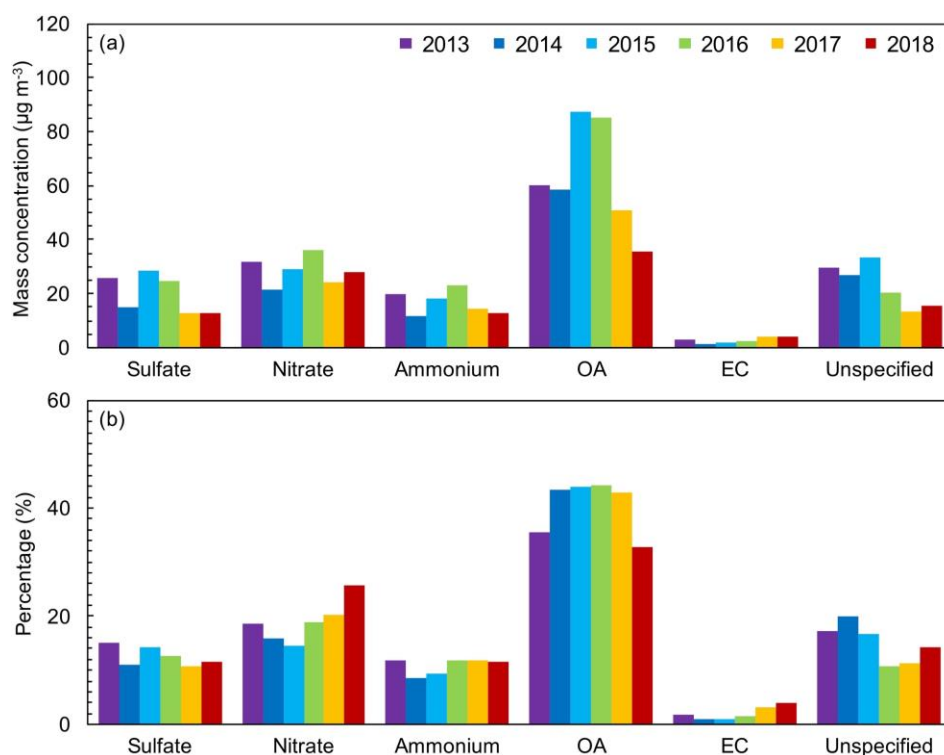


Figure 1. Variations of the filter measured average (a) mass concentrations of the PM_{2.5} constituents and (b) their contributions to the PM_{2.5} mass at an urban site in Beijing from 2013 to 2018 during wintertime PM pollution days with PM_{2.5} concentrations exceeding 75 µg m⁻³.

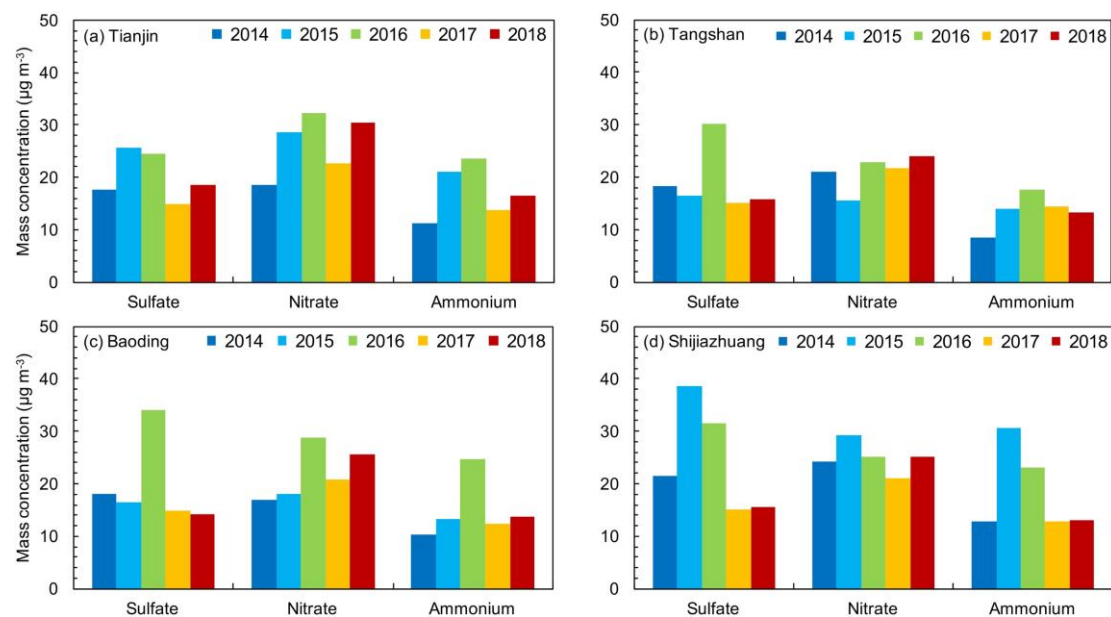


Figure 2. Variations of the filter measured wintertime sulfate, nitrate, and ammonium concentrations from 2014 to 2018 when the $\text{PM}_{2.5}$ level exceeds $75 \mu\text{g m}^{-3}$ in (a) Tianjin, (b) Tangshan, (c) Baoding and (d) Shijiazhuang in the BTH.

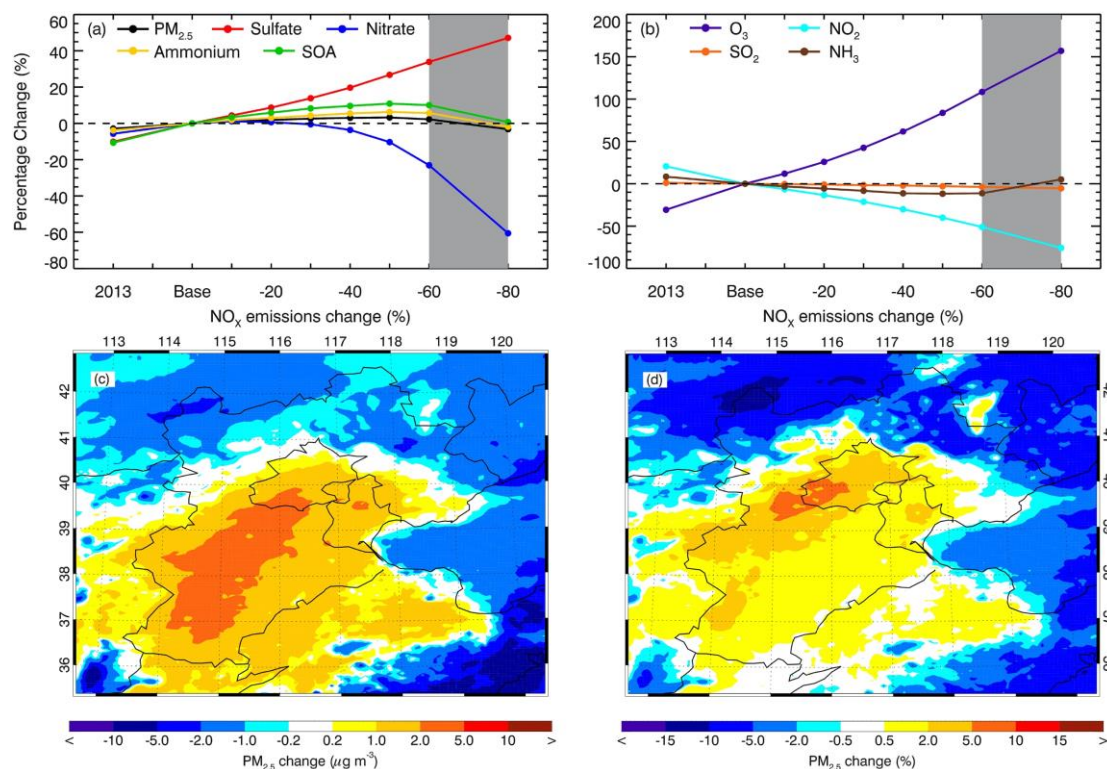


Figure 3. Variations of average concentrations of PM_{2.5} and secondary aerosols (a) as well as the gas pollutants (b) in the BTH during the episode with the NO_x emissions changes, and mass (c) and percentage (d) distributions of the PM_{2.5} variation during the simulation period when the NO_x emissions are reduced by 50%. The shading area in (a) and (b) shows the scenario of the NO_x emission reduction during the lockdown period due to the COVID-19 outbreak.

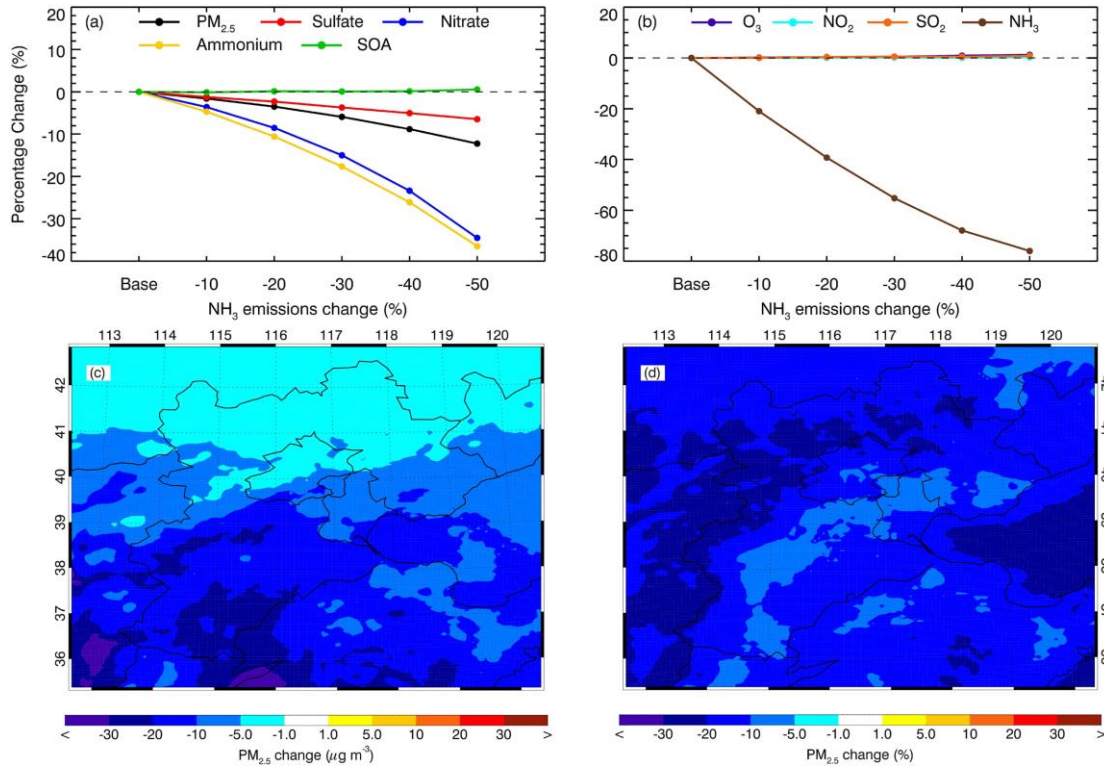


Figure 4. Variations of average concentrations of $\text{PM}_{2.5}$ and secondary aerosols (a) as well as the gas pollutants (b) in the BTH during the episode when the NH_3 emissions are reduced from 10% to 50%, respectively, and mass (c) and percentage (d) distributions of $\text{PM}_{2.5}$ reductions when the NH_3 emissions are reduced by 50%.